Pla, L.; Santiago Felipe, S.; Tormo-Mas, MÁ.; Pemán, J.; Sancenón Galarza, F.; Aznar, E.; Martínez-Máñez, R. (2020). Aptamer-Capped nanoporous anodic alumina for Staphylococcus aureus detection. Sensors and Actuators B Chemical. 320(128281). https://doi.org/10.1016/j.snb.2020.128281

# Aptamer-Capped Nanoporous Anodic Alumina for *Staphylococcus aureus* Detection

Luis Pla[a,b,c,‡], Sara Santiago-Felipe[a,b,c,‡], María Ángeles Tormo-Más[d*], Javier Pemán[d,e], Félix Sancenón[a,b,c,f], Elena Aznar[a,b,c,f*], and Ramón Martínez-Máñez[a,b,c,f*]

[a] CIBER de Bioingeniería, Biomateriales y Nanomedicina (CIBER-BBN), Spain.

[b] Instituto Interuniversitario de Investigación de Reconocimiento Molecular y Desarrollo Tecnológico, Universitat Politècnica de València, Universitat de València, Camino de Vera s/n, 46022, Valencia, Spain.

[c] Unidad Mixta de Investigación en Nanomedicina y Sensores. Universitat Politècnica de València, Instituto de Investigación Sanitaria La Fe, Valencia, Spain

[d] Grupo Acreditado de Infección Grave. Instituto de Investigación Sanitaria La Fe, Avenida Fernando Abril Martorell, 46026, Valencia, Spain.

[e] Servicio de Microbiología Hospital Politècnic i Universitari La Fe. Instituto de Investigación Sanitaria La Fe, Avenida Fernando Abril Martorell, 46026, Valencia, Spain.

[f] Unidad Mixta UPV-CIPF de Investigación en Mecanismos de Enfermedades y Nanomedicina. Universitat Politècnica de València, Centro de Investigación Príncipe Felipe, Valencia, Spain.

‡ These authors contributed equally

[*] Corresponding author:
E-mail: elazgi@upvnet.upv.es; tormo_man@iislafe.es; rmaez@upvnet.upv.es

**Abstract**

The development of new detection systems for an accurate and rapid identification of pathogens has become an essential challenge in the biomedical field. Herein a highly selective platform based on aptamer-gated nanomaterials for specific *Staphylococcus aureus* detection is presented. In the proposed design, a nanoporous anodic alumina (NAA) scaffold is loaded with the fluorescent indicator rhodamine B, while pores entrances are capped by a DNA aptamer which selectively recognizes *S. aureus* cells in less than 1 hour. When *S. aureus* cells are present, the solid is selectively uncapped, and the dye is released to the medium. This nanodevice allows the detection of bacterial concentrations between 2 and 5 CFU $mL^{-1}$ (in buffer and blood, respectively) and it has demonstrated excellent behavior in terms of specificity and robustness. A set of 25 different clinical samples are analyzed using this simple procedure obtaining excellent results, which agree with conventional hospital reference techniques for the identification of *S. aureus*. This new method is sensitive, rapid and low cost, and avoids steps such as polymerase chain amplification reaction, which makes it suitable for use in point-of-care detection systems.

**Keywords**

aptamers, gated materials, *Staphylococcus aureus*, optical sensors

## 1. Introduction

*Staphylococcus aureus* is a Gram-positive and facultative anaerobic bacterium, and it is considered as one of the most important human pathogens. Although it is not always pathogenic, the existence of *S. aureus* is highly common in the environment and can cause numerous diseases, from mild skin infections to life-threatening complications. Moreover, it is one of the most important causes of nosocomial contagions and it is often the cause of wound infections after surgical interventions [1].

*S. aureus* has been traditionally identified by detection methods that involve culture growing, colony isolation and different serological and biochemical tests. More recently, several works have focused on the advancement of detection strategies based on the biomolecular recognition of *S. aureus*, including amplification reactions such as

polymerase or ligase chain reactions, strand displacement amplification or enzyme-linked immunosorbent assay [2-5]. Although these techniques usually show high sensitivity and selectivity, their complexity, cost and time of analysis, have limited their widespread application for clinical diagnosis.

Biosensor-based technologies have demonstrated an enormous potential for the recognition of toxins, pathogens and other biomolecules in a rapid, sensitive and reproducible way [6, 7]. Different methods using surface plasmon resonance, fluorescence, colorimetric, electrochemical or light scattering signals have been described for *S. aureus* bacterium detection [8, 9]. In most cases, antibodies are used as a recognition element. Antibody-based immunosensors have demonstrated high specificity and have been well-established [10, 11]. However, the use of antibodies could encounter some limitations due to their low stability, high cost and complicated modification and functionalization. In this context, aptamers are other class of high-affinity molecules that have provided excellent results for the recognition of a great variety of analytes in the biotechnological field [12-15]. Aptamers are single-chain nucleic acids (RNA or DNA) that are generally *in vitro* synthesized through the known process of "Systematic Evolution of Ligands by EXponential enrichment" (SELEX). They have shown affinities for their targets similar or higher than that obtained by most of the reported monoclonal antibodies, presenting dissociation constants from the picomolar to low micromolar ranges. Furthermore, aptamers are easy to modify, easily scalable for chemical synthesis of large quantities of product and stable for long term storage [16]. Recently, some sequences of aptamers have been chosen and used for the specific recognition of bacteria including *Bacillus anthracis, Escherichia coli, Salmonella enterica, Mycobacterium tuberculosis* or *Staphylococcus aureus*. Nevertheless, none of these works was capable of identifying the bacteria at low concentrations without a previous DNA amplification reaction [8, 9, 17].

Progress in nanotechnology has significantly increased the number of possibilities for biosensors development. A key issue in this field is the design of new hybrid organic-inorganic materials that combine, in a single entity, the potential of nanomaterials with the recognition, sensitivity and selectivity capabilities of biomolecules. The anchoring of a variety of supramolecules, biomolecules or organic molecules onto several inorganic scaffolds with diverse chemical nature, size or shape, has allowed the

development of a great variety of smart nanodevices as probes that have demonstrated advantages such as rapidity, simplicity and sensitivity [17-19]. In this context, several works have been recently published that combine nanomaterials and the use of aptamers to develop different methods for *S. aureus* detection [9, 21-23]. In these studies, nanodevices are mainly used to pre-concentrate bacteria cells as a previous step to further detection by optical systems. For example, Kurt *et al*. (2016) developed quantum dots functionalized with aptamer and upconverting nanoparticles for the luminescent identification of *S. aureus* reaching a limit of detection of 16 CFU $mL^{-1}$ [21]. In another work, few tens of *S. aureus* cells were detected by combining functionalized gold nanoparticles with surface-assisted laser desorption and ionization mass spectrometry [22]. Likewise, Wang *et al*. achieved the recognition of 10 CFU $mL^{-1}$ of *S. aureus* using a biosensor based on the magnetically assisted Surface-Enhanced Raman Scattering technology [9]. A simple detection system able to recognize the bacterium and provide a signal in several minutes could facilitate the essay and deliver a highly valuable information in a shorter period of time, which directly affects patients' disease evolution.

Porous materials provided with "molecular gates" have been widely applied in direct detection and diagnosis systems based on stimuli-response methods. In these gated-materials, fluorescent dye rhodamine B is encapsulated into the porous support structure, and the capping mechanism is designed so that the release of the cargo is only induced when the target analyte is present [19, 24, 25]. Following this mechanism, gated systems have been recently developed for the selective detection of cations, anions, neutral molecules and biomolecules [18, 26, 27]. Among supports used in gated sensing protocols, nanoporous anodic alumina (NAA) has arisen as a promising material thanks to its wide variety of applications [28-31]. NAA supports are stable, do not degrade in aqueous solutions and can be reused several times after calcination treatment. NAA supports have demonstrated excellent performances in sensing applications using nucleic acids (DNA, RNA or aptamers) as molecular gate [32, 33, 34]. Nevertheless, as far as we are aware, no aptamer-capped NAA system dedicated to bacterial optical detection has been reported yet.

Based on what has been mentioned above, a new hybrid gated nanostructured sensor for the fluorogenic identification of *S. aureus* cells is presented. In the proposed system the

NAA scaffold is charged with the rhodamine B and capped with an aptamer specific of *S. aureus* cells. The capping aptamer blocks the pores and inhibits the fluorophore release. The recognition mechanism is such that if the analyte is present, the aptamer is selectively displaced, with the subsequent pore opening and cargo delivery. The proposed gated materials are characterized and employed for the recognition of *S. aureus* bacteria in real clinical samples from infected patients, obtaining results in less than an hour.

## 2. Materials and methods

### 2.1 General Techniques

A ZEISS Ultra 55 microscope was employed to perform Field Emission Scanning Electron Microscopy (FSEM) and Energy Dispersive X-ray spectroscopy (EDX) analyses. Measurements of fluorescence spectroscopy were carried out on a Synergy H1 microplate reader (BioTek, Winooski, VT, USA).

### 2.2 Chemicals

3-(Triethoxysilyl)propyl isocyanate, rhodamine B, tris(hydroxymethyl)aminomethane (TRIS), triethylamine (TEA), and hydrochloric acid were obtained from Sigma-Aldrich Química (Madrid, Spain). Oligonucleotide ($NH_2$-$(CH_2)_6$-5'-AAA AAA CCC CCC-3') and the aptamer (**O1)** and (5'-TTT TGG GGG GTC CCT ACG GCG CTA ACC CCC CCA GTC CGT CCT CCC AGC CTC ACA CCG CCA CCG TGC TAC AAC GGG GGG TTT T-3') (**O2**) were purchased from Invitrogen by Thermo Fisher Scientific (Madrid, Spain). NAA scaffolds were purchased from InRedox (CO, USA).

### 2.3 Synthesis of materials S1, S2 and S3

In a conventional synthesis of material **S1**, 8 independent NAA supports of 2 mm of diameter were submerged in a mixture of rhodamine B dye in $CH_3CN$ (18.6 mg, 1 mM, 8 mL). To enable the loading of the pores, the solution was agitated for 24 h. Then, the surface of the support was functionalized by the addition of (3-(triethoxysilyl)propyl isocyanate (0.01 mmol, 328 μL) and stirring the mixture for 6 h.

For the preparation of **S2**, **S1** was immersed in a mixture of rhodamine B in $CH_3CN$ (1 mM, 700 μL), and then 100 μL of the oligonucleotide **O1** (10 μM) and 2 μL of TEA were dropped. Then, the solution was mixed for 3 h at room temperature.

To prepare **S3**, **S2** was immersed with 90 μL of PBS buffer and oligonucleotide **O2** was added (10 μL, 100 μM). The suspension was agitated for 2 h at 30 ºC, and the obtained nanomaterial was washed dropwise with PBS buffer (phosphate-buffered saline, pH 7.5) to eliminate the unattached oligonucleotide.

### 2.4 Bacterial growth

The main bacterial strains employed in this work were *Staphylococcus aureus* (RN4220 strain) [35], *Staphylococcus conhii* (SCN123 strain) [36], *Staphylococcus capitis* (IPA57 strain) [36], *Staphylococcus epidermidis* (RP62A strain) [37], *Staphylococcus carnosus* (TM300 strain) [38], *Staphylococcus saprophyticus* (SCN159 strain) [35], *Staphylococcus chromogenes* (C483 strain) [39], *Staphylococcus xylosus* (C482 strain) [39], *Staphylococcus haemolyticus* (IPA71 strain) [36], *Staphylococcus lugdunensis* (IPA26 strain) [36], *Staphylococcus hominis* (SCN4 strain) [36], *Staphylococcus warneri* (SCN44 strain) [36]. All bacteria were cultured in tryptic soy broth medium (TSB) or agar plates (TSA) and were grown at 37 °C for 24 hours. The bacteria concentration was calculated by determining the optical density at 600 nm, given that $OD_{600}$ = 1.0 corresponds to $1.5 \cdot 10^8$ CFU $mL^{-1}$. 100 μL were grown in TSA plates to check that the experiments were carried out with the corresponding inoculum concentration.

### 2.5 Assay Protocol

Solids' behavior were evaluated by measuring the emitted fluorescence of rhodamine B delivered from the pores in the presence of *S. aureus* cells. In a common experiment, two independent **S3** nanomaterials were submerged in 900 μL of PBS. Then, 100 μL of an *S. aureus* suspension ($10^3$ CFU $mL^{-1}$) was inoculated to only one of the supports while 100 μL of buffer was transferred to the other. Both solutions were stirred at 25 ºC,

and aliquots were obtained at scheduled times. Finally, dye released was determined by registering the fluorescence of the indicator in the solution at 575 nm ($\lambda_{exc}$ = 555 nm).

### 2.6 Real Media Experiments

The applicability of the method in a more realistic context was tested. For that, 400 µL of different competitive media (serum, pleural, peritoneal, synovial or cerebrospinal fluid) were artificially inoculated with *S. aureus* (100 µL, $10^3$ CFU $mL^{-1}$) and added to independent **S3** supports in a final volume of 1 mL. Solutions were maintained at 25 ºC, and rhodamine B released from the porous was measured at 575 nm ($\lambda_{exc}$ = 555 nm) after 60 min.

### 2.7 Quantification of the loaded dye

In order to estimate the amount of the Rhodamine B that can be loaded in the pores, two individual **S3** solids were submerged in 1000 µL of PBS. Then, one of them was stirred at 90 °C during 60 min to force the opening of the pores and the maximum cargo release, and the other was maintained in agitation at 25 °C during 60 min as a control. The delivered fluorophore was observed at 575 nm ($\lambda_{exc}$ = 555 nm), and the experiment was done by triplicate. Quantification of final released dye was undertaken using a calibration curve with different concentrations of rhodamine B.

### 2.8 Amplification Assay

In order to calculate the amplification of the signal, two individual **S3** solids were submerged in 900 µL of PBS. Then, 100 µL of an *S. aureus* suspension ($10^3$ CFU $mL^{-1}$) was inoculated to one of them and 100 µL of buffer was added to the other. Both solutions were stirred at 25 °C during 60 min and the delivered fluorophore was observed at 575 nm ($\lambda_{exc}$ = 555 nm). Quantification of finally released dye was undertaken using a calibration curve with different concentrations of rhodamine B, to then directly correlate with the number of CFU $mL^{-1}$ that opened the system.

### 2.9 Response vs concentration experiments

The response of the material to different decreasing concentrations of *S. aureus* was evaluated and compared in both buffer and blood media. For that, 500 µL of 10-fold dilutions of *S. aureus* suspensions ($10^3$ – 0 CFU $mL^{-1}$) were added to seven independent **S3** supports in a final reaction volume of 1 mL of PBS or non-contaminated blood. After 60 min at 25 ºC rhodamine B released from the porous was measured at 575 nm ($\lambda_{exc}$ = 555 nm).

### 2.10 Selectivity

The selectivity of the nanosensor was determined by performing the same delivery experiments in the presence of other *Staphylococcus* species and different mixtures of them (*S. conhii*, *S. capitis*, *S. epidermidis*, *S. carnosus*, *S. saprophyticus*, *S. chromogenes*, *S. xylosus*, *S. haemolyticus*, *S. lugdunensis*, *S. hominis*, *S. warneri and a mixture of S. aureus* and *S. carnosus*, a mixture of *S. aureus*, *S. hominis* and *S. capitis*, and a mixture of *S. conhii* and S. *warneri*). For that, 100 µL of a bacterial suspension of each specie ($10^3$ CFU $mL^{-1}$) were added to fifteen independent **S3** supports in a final reaction volume of 1 mL of PBS. After 60 min at 25 ºC rhodamine B released from the pores was measured at 575 nm ($\lambda_{exc}$ = 555 nm).

### 2.11 Validation in Clinical Real Samples

Probe performance was evaluated in real clinical samples from patients. Twenty-five blood culture samples were examined using the automated BacT/ ALERT VIRTUOTM system (bioMérieux, Madrid, Spain). Positive bottles were subcultured in chocolate agar plates (bioMérieux) for 24 hours, and definitive identification of *S. aureus* isolates was carried out by MALDI-TOF Mass Spectrometry (VITEK MS, bioMérieux). In parallel, for each sample, 500 µL of blood culture from infected and non-infected patients was added to independent **S3** supports in a final reaction volume of 1 mL of PBS and the rhodamine B delivered from the support was measured after 60 min at 25 ºC.

### 2.12 Ethical Committee

The present study was approved by the Ethics Committee of Hospital Universitari i Politècnic La Fe (2017/0370).

## 3. RESULTS AND DISCUSSION

### 3.1 Development and characterization of the sensing system

The developed sensing system consists of a nanoporous NAA scaffold in which the pores were loaded with the fluorophore rhodamine B. The outer surface was functionalized with the organic linker 3-(triethoxysilyl)propyl isocyanate to allow the covalently anchoring of the capping DNA molecules by the formation of urea bonds with the short oligonucleotide $NH_2$-$(CH_2)_6$-5'-AAA AAA CCC CCC-3' (**O1**), which is designed to recognize and hybridize with the sequence 3'-TTT TGG GGG G-5'. The oligonucleotide 5'-TTT TGG GGG GTC CCT ACG GCG CTA ACC CCC CCA GTC CGT CCT CCC AGC CTC ACA CCG CCA CCG TGC TAC AAC GGG GGG TTT T-3'(**O2**), which contains the specific sequenceto recognize *S. aureus* cells (i.e. 5'-TCC CTA CGG CGC TAA CCCCCC CAG TCC GTC CTC CCA GCC TCA CAC CGC CAC CGT GCT ACA AC-3'), was employed to block the pores by hybridization with **O1**, obtaining the final sensing gated nanomaterial **S3** (Figure 1).
In the absence of target analyte, the dsDNA **O1**-**O2** anchored to the external surface of the inorganic scaffold was expected to be bulky enough to block pores and to inhibit dye delivery. On the contrary, due to the higher affinity of the aptamer for *S. aureus* cells than for **O1**, it was expected that in the presence of the target bacteria, the aptamer would selectively be displaced from the surface resulting in *S. aureus*-aptamer binding, pore opening and dye release.

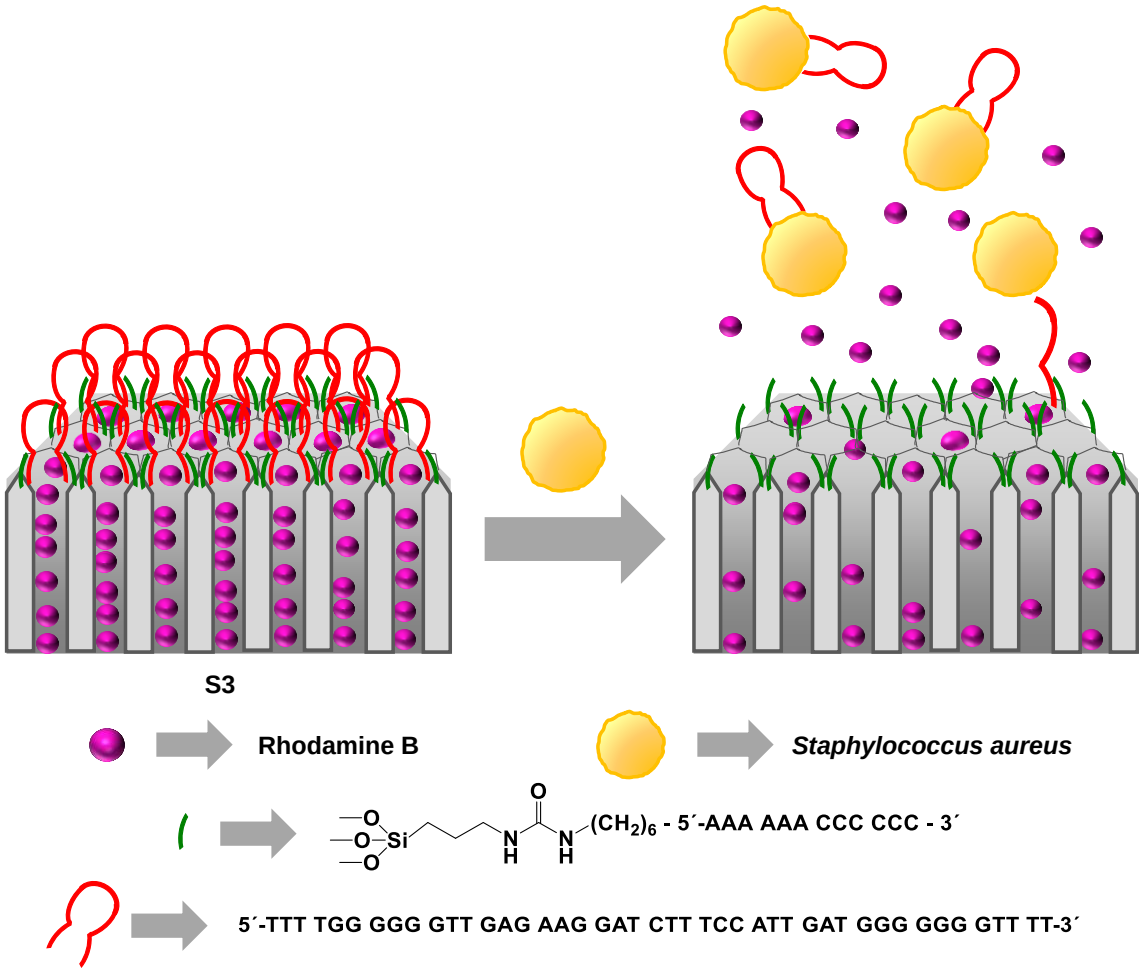


**Figure 1.** Scheme of the capped NAA material **S3** selective performance in the presence of *S. aureus* cells. In the lack of *S. aureus,* pores are blocked while in the presence of bacteria, the cell interacts with the aptamer allowing oligonucleotide displacement and delivery of the entrapped dye.

The starting NAA scaffold and the obtained **S1**, **S2** and **S3** supports were characterized by FESEM and EDX analysis. The NAA support (InRedox®) consisted on anodic aluminum oxide film grown on a 0.1 mm thick aluminum layer with a pore density of $9 \cdot 10^{11}$ $cm^{-2}$. Pores entrance present a funnel-like shape which gradually switches from a larger size (20-30 nm) at the top of the funnel to a 5 nm size at the end. Transition from one size to another extends to a profundity of approximately 3 times the pore diameter, and below this depth, the pore structure becomes uniform along 10 µm. With this pore morphology, the maximum amount of cargo that is possible to load and release was estimated to be 4 ng of Rhodamine B per µg of NAA.

The FESEM images of the starting NAA confirmed the described structure. Representative images of solid **S2** showed the same porous structure as the parent material. FESEM images of material **S3** revealed the existence of an organic covering on the top of the pores. In contrast, the visualization of the porous configuration in specific areas confirmed the preservation of the nanoporous structure in **S3** (Figure 2). Organic content in **S1**, **S2** and **S3** was analyzed by energy-dispersive X-ray spectroscopy (Table 1). As expected, high carbon content (C/Al 1.424) was found in solid **S1**, due to the high loading capacity of NAA material. Solid **S2** showed a decrease of carbon content due to the experimental conditions for **O1** attachment, which do not prevent a partial cargo release (C/Al 0.624). Finally, solid **S3** presented a slight increase in organic matter content (C/Al 0.704) that can be associated with an effective capping of the support with the oligonucleotide **O2**. Likewise, the presence of nitrogen and phosphorous atoms from the capping oligonucleotide in the final material was confirmed.

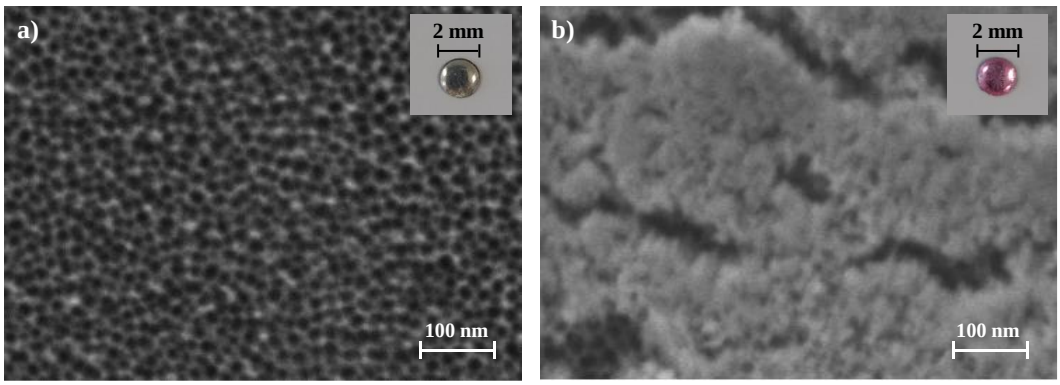


**Figure 2**. FESEM images of NAA support (a) and solid **S3** (b). Insets: Digital photographs of the corresponding solids

**Table 1.** Atomic elements relation in the different prepared solids.

| | C/Al | N/Al | P/Al |
|---|---|---|---|
| **S1** | 1.424 ± 0.030 | - | - |
| **S2** | 0.624 ± 0.008 | ND | ND |
| **S3** | 0.704 ± 0.021 | 0.044 ± 0.004 | 0.012 ± 0.003 |

### 3.2. Delivery kinetics

The *S. aureus* recognition through solid **S3** mechanism is founded on the opening of the gated nanomaterial in the presence of the bacteria that leads to selective rhodamine B delivery. The response of **S3** to *S. aureus* was studied employing a bacterial suspension of $10^3$ CFU $mL^{-1}$. To conduct this experiment, two separated gated **S3** supports were immersed in PBS buffer (pH 7.5). Then, 100 μL of the bacterial suspension was transferred to one of the materials (final *S. aureus* concentration of $10^2$ CFU $mL^{-1}$), and 100 μL of PBS was added to the other. To calculate the delivered dye in the aqueous phase, the fluorescence of the aliquots taken at predetermined times was measured. As depicted in Figure 3, in the absence of the bacteria, little rhodamine B emission was recorded, which is suggestive of notable pore closure by the dsDNA **O1**-**O2** anchored to the surface of the scaffold (curve a). On the contrary, when *S. aureus* cells were present, a remarkable dye diffusion to the aqueous solution was registered (Figure 3, curve b). The observed enhancement in fluorescence emission was attributed to the migration of capping aptamers from **S3** support to the solution as a result of a specific interaction with the bacteria cell. It is worth mentioning that in previous works the binding capacity of the aptamer for *S. aureus* cells, measured as dissociation constant, was 35 nM [23], which is indicative of a high aptamer-bacteria affinity and it is in accordance with our results.

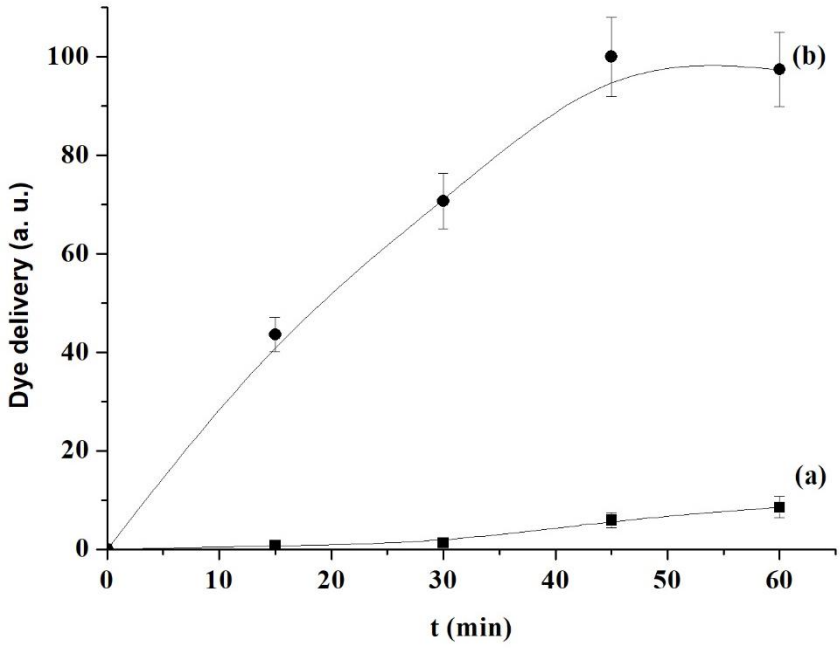


**Figure 3**. Rhodamine B delivery from the pores of material **S3** in PBS buffer (pH 7.5) at different periods of time. Curve (a) indicates dye release in the lack of *S. aureus* cells

and curve (b) represents cargo delivery in the presence of target *S. aureus* at a concentration of $10^2$ CFU $mL^{-1}$.

### 3.3. Analytical performance: sensitivity, specificity and robustness studies

The sensitivity of the method was determined by submitting the support to different concentrations of *S. aureus* and studying the response generated. For that, 6 independent **S3** supports were immersed in PBS, and 100 μL of 10-fold bacterial suspension dilutions were added to each material, reaching a range of final concentrations between $10^3$ and $10^{-5}$ CFU $mL^{-1}$. After 60 min, the total sum of rhodamine B diffused to the aqueous phase was measured. Results showed that delivered dye was directly related to *S. aureus* concentration, upholding the sensing protocol detailed above (Figure 4A). A limit of detection (LOD) of 2 CFU $mL^{-1}$ was calculated based on the intersection point of the two slopes of the represented curve. This LOD value is equivalent to those obtained by most aptamer-based nanosystems described in the literature for *S. aureus* detection [8, 9,17, 22, 23]. Providing similar sensitivity, the presented nanosensor is also simpler and faster (ca. 60 min). Moreover, in the proposed system, amplification takes place in the signalling step and not in the recognition event, which is a substantial improvement in the progress of sensing systems technology. Specifically, in gated materials, the recognition mechanism is separated from the signalling event, having an independent stoichiometric relation. This implies that the aptamer-bacteria recognition involves the liberation of a large amount of reporter molecules. In the presented system, it was found that 10 CFU $mL^{-1}$ of *S. aureus* was capable of release an average of $5 \cdot 10^{12}$ molecules of rhodamine B, which means a signal amplification of $10^{11}$ reporter molecules per recognized bacteria. This signal amplification depends both on the geometry of the pores, which will determine the amount of cargo loaded, and on the affinity of the probe for the target, which will determine the efficiency of opening the pores. In line with this, published works have estimated that a single *S. aureus* cell can bind from 900 to 1200 aptamer molecules, which may contribute to that high signal amplification [23].

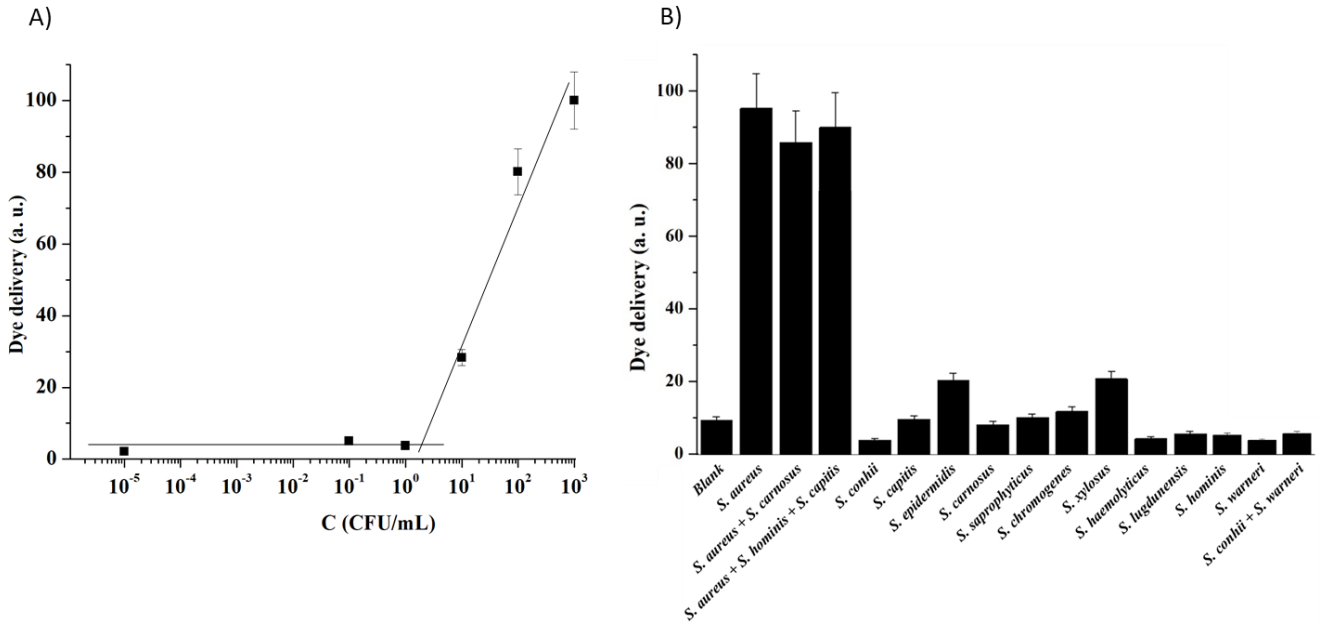


**Figure 4**. Dye release from solid **S3** (A) in the presence of decreasing amounts of *S. aureus*; (B) in the presence of $10^2$ CFU $mL^{-1}$ of *S. aureus*, a mixture of *S. aureus* + *S. carnosus*, a mixture of *S. aureus* + *S. hominis* + *S. capitis*, *S. conhii*, *S. capitis*, *S. epidermidis*, *S. carnosus*, *S. saprophyticus*, *S. chromogenes*, *S. xylosus*, *S. haemolyticus*, *S. lugdunensis*, *S. hominis*, *S. warneri* and a mixture of *S. conhii* + S. *warneri.* Assays were carried out at 60 min in PBS buffer at pH 7.5.

Additionally, the specificity of the nanomaterials was assessed by testing the response of **S3** to other *Staphylococcus* species (*S. conhii*, *S. capitis*, *S. epidermidis*, *S. carnosus*, *S. saprophyticus*, *S. chromogenes*, *S. xylosus*, *S. haemolyticus*, *S. lugdunensis*, *S. hominis* and *S. warneri*) and mixtures of some of them (*S. aureus* + *S. carnosus*, *S. aureus* + *S. hominis* + *S. capitis* and *S. conhii* + S. *warneri*) (Table 2). For that, the dye delivered from 15 independent **S3** supports was monitored in the presence of $10^2$ CFU $mL^{-1}$ of each bacterium. As it is depicted in Figure 4B, *S. aureus* was the only microorganism capable of producing a remarkable dye release. It should be noted that the selective aptamer-cell recognition, and therefore the measured fluorescence, was not affected by the presence of other microorganisms in the media, indicating the absence of interference. On the other hand, all the other *Staphylococcus* species induced fewer pore uncapping and less cargo delivery, which demonstrates the capacity of the system to selectively discriminate between *S. aureus* and other *Staphylococcus* species.

In addition, to evaluate the robustness of the system, the behavior of **S3** to the presence of 100 µL of $10^3$ CFU $mL^{-1}$ of *S. aureus* was evaluated in different clinical relevant media (serum, pleural, peritoneal, synovial and cerebrospinal fluid). As it is depicted in Figure 5, the presence of *S. aureus* cells produced a selective displacement of the aptamer, pore uncapping and dye delivery in all tested media. Moreover, although a slightly higher residual release was observed in competitive media than in buffer (20% vs 5%), the measured fluorescence in the presence of bacteria cells was comparable to that achieved in PBS buffer (ca. 60-80%). Likewise, the possibility to directly detect *S. aureus* using the gated material **S3** was investigated. Taking into account the usual bloodstream *S. aureus* concentration (1-$10^3$ CFU $mL^{-1}$), aliquots of fresh blood were inoculated with different amounts of *S. aureus* (0, $2\cdot10^{-6}$, $2\cdot10^{-3}$, $2\cdot10^{-1}$, 20, $2\cdot10^2$ and $2\cdot10^3$ CFU $mL^{-1}$, respectively) to emulate *S. aureus* contaminated blood. Then, 500 µL of each sample was added to an Eppendorf tube containing the **S3** support and 500 µL of PBS buffer. After 60 min at 25 ºC rhodamine B released from pores was registered at 575 nm ($\lambda_{exc}$ = 555 nm). As depicted in Figure 5B, released rhodamine B was proportional to the analyte concentration and, based on the intersection point of the two slopes of the curve, a LOD of 5 CFU $mL^{-1}$ was calculated. This LOD is in the same order of magnitude as that obtained in buffer media, demonstrating its high potential of the probe for clinical applications without the need of previous culture, sample treatment or amplification steps. Moreover, preliminary studies carried out to assess the stability of aptamer-gated nanomaterials have demonstrated that this type of nanosensors can be stored up to 12 weeks without any changes in their sensing performance [27].

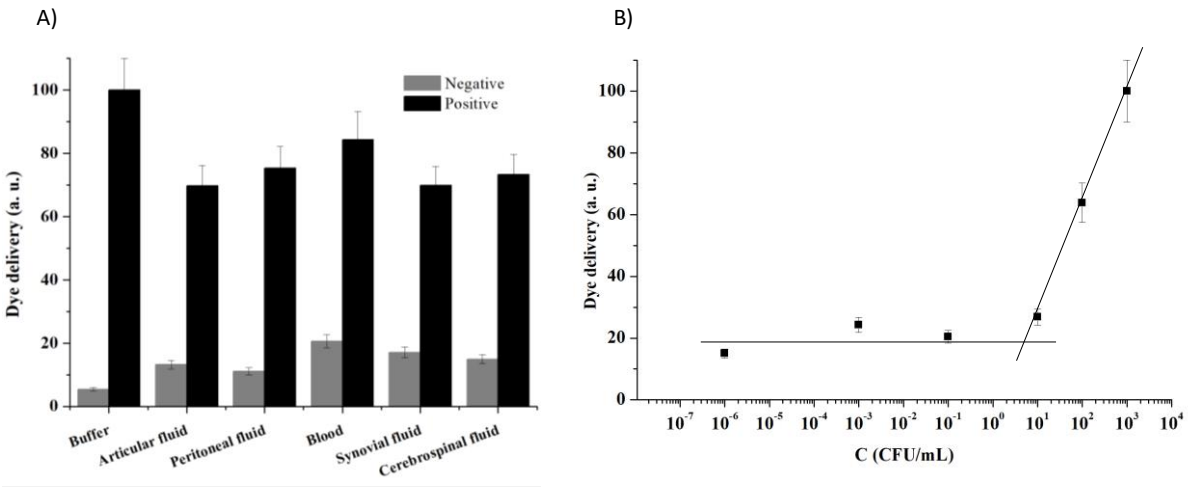


**Figure 5**. Delivery of rhodamine B from material **S3** (A) in diverse clinical media with $10^2$ CFU $mL^{-1}$ of *S. aureus*, and (B) in the presence of decreasing concentrations of *S. aureus* cells in blood. Assays took place at 60 min in PBS buffer at pH 7.5.

### 3.4. *S. aureus* detection in clinical samples

The detection of *S. aureus* cells directly in clinical samples is crucial for the successful application of the probe in the real medical practice. Hence, the applicability of the sensing materials to detect *S. aureus* from infected samples was studied. The current reference method for *S. aureus* detection in most hospitals is based on specimen culture attached to subsequent identification techniques. In the first step, the clinical sample is cultured using automated culture equipment until bottles are detected as positive ($10^6$-$10^8$ CFU $mL^{-1}$), which takes around 12 h. Then, a gram stain is performed with a sub-sample from the bottle to confirm the presence of microorganisms and to determine its morphotype. Subsequently, a sample from the positive bottle is subcultured in chocolate agar, and after 24 h more, *S. aureus* colonies are identified by MALDI-TOF MS. The total time until *S. aureus* identification could range between 36 h to several days [40-44].

In the present work, 25 clinical blood samples from Hospital Universitari i Politècnic La Fe from *S. aureus* infected and noninfected patients were analyzed. These samples were managed by the standard procedure that is automated blood culture, subsequent subculture and *S. aureus* identification by MALDI-TOF Mass Spectrometry. In parallel, the same 25 samples were assessed by triplicate by using the gated material **S3**. For that, 25 individual **S3** supports were immersed in 500 μL PBS, and 500 μL of blood culture

was added to each one. As in previous experiments, released rhodamine B was measured by fluorescence after 30 min. Results showed a total coincidence between the current reference methods for *S. aureus* in hospitals and our procedure using **S3** in the 25 analyzed samples. In the course of the study, one sample was negative for *S. aureus* but positive for *S. lugdunensis* (Table 2). Based on these results, our system is demonstrating a sensitivity of 100% and positive and negative predictive values of 100%. The high competitiveness of the gated materials compared to the conventional reference methods is remarkable, providing high accuracy, easiness to use, rapidity and lower cost. In addition, a final confirmation experiment was performed. All **S3** evaluation studies, prior clinical validation, were performed using *S. aureus* RN4220 strain. However, in the clinical context, other *S. aureus* strains can be found in *S. aureus* infected samples. To confirm that the method was able of detect *S. aureus* in blood samples at a lower concentration than in blood culture (avoiding bacterial growth), the same 25 samples of the study were grown in TSB media and diluted to a concentration of $10^3$ CFU $mL^{-1}$. Then, **S3** supports were immersed in a solution of PBS-blood (50% v/v) and then 100 μL of the bacterial dilution was added to each one (final concentration of $10^2$ CFU $mL^{-1}$). Results showed a positive rhodamine B release for all the *S. aureus*-containing samples independently of the strain, demonstrating the ability of the developed system to recognize a variety of different *S. aureus* strains at a lower concentration than in blood culture.

**Table 2.** Results from blood samples analyzed using the gated material **S3** and the reference blood culture technique.

| # Sample | Reference method (blood culture)[a] | **S3**[b] |
|---|---|---|
| 1 | + | + |
| 2 | + | + |
| 3 | + | + |
| 4 | + | + |
| 5 | + | + |
| 6 | + | + |
| 7 | + | + |
| 8 | + | + |
| 9 | + | + |
| 10 | + | + |
| 11 | + | + |
| 12 | + | + |
| 13 | + | + |
| 14 | + | + |

| | | |
|---|---|---|
| 15 | + | + |
| 16 | + | + |
| 17 | + | + |
| 18 | + | + |
| 19 | -[c] | - |
| 20 | - | - |
| 21 | - | - |
| 22 | - | - |
| 23 | - | - |
| 24 | - | - |
| 25 | - | - |

[a)] Positive (+) means that any *S. aureus* colony was isolated from blood samples.

[b)] Positive (+) means that the fluorescence intensity at 575 nm ($\lambda_{exc}$ = 555 nm) was equal or higher than 3-fold the standard deviation of three negative controls.

[c)] Negative for *S. aureus* but positive for *S. lugdunensis*.

## 4. Conclusion

Herein, we demonstrate that nanoporous materials and a suitable aptamer can be combined to obtain a sensitive, robust and competitive fluorogenic sensor for *S. aureus* detection in clinical blood samples. The probe consists of an NAA scaffold previously charged with the fluorescent dye rhodamine B and blocked with a selective aptamer for *S. aureus*. The presence of the bacteria results in the migration of capping aptamer, pore opening and release of the fluorophore. The probe shows a limit of detection of 2 CFU $mL^{-1}$ in PBS buffer and 5 CFU $mL^{-1}$ in blood media, which are equivalent to other *S. aureus* state-of-the-art reported detection systems. Moreover, the probe demonstrates a high selectivity to *S. aureus* and does not respond to the presence of other *Staphylococcus* species. Using this simple method, the probe is applied to the identification of *S. aureus* in clinical samples with very good results in terms of sensitivity and predictive values. The proposed method is simple, fast, and portable, and it can be easily modified by using different reporters and capping sequences. It also may inspire the development of new simple tests that offer a great potential for point-of-care pathogen testing.

## Acknowledgements

This study was supported by the Spanish Government (projects RTI2018-100910-B-C41 and SAF2017-82251-R (MCUI/AEI/FEDER, UE)), the Generalitat Valenciana (project PROMETEO/2018/024), the Universitat Politècnica de València−Instituto de Investigación Sanitaria La Fe (B02-MIRSA project) and CIBER-BBN (NANOPATH and valorization project CANDI-EYE). S.S. thanks the Instituto de Salud Carlos III and the European Social Fund for the financial support "Sara Borrell" (CD16/000237). L.P. thanks to Ministerio de Economia, Industria y Competitividad for his FPI grant. The authors are grateful for the professional English language editing to Mr. Arash Javadinejad, English Instructor and pubication Editor at the Instituto de Investigación Sanitaria La Fe, Valencia, Spain.

## Supplementary Material

Supplementary material about experimental and characterization details is available in the online version of this article at http://dx.doi.org/10.1007/s12274-***-****-* (automatically inserted by the publisher).

## Declaration of competing interest

The authors declare that they have no known competing financial interests or personal relationships that could have appeared to influence the work reported in this paper.

## CRediT authorship contribution statement

Luis Pla: Investigation; Methodology; Writing - original draft, Sara Santiago-Felipe: Investigation; Methodology; Writing - original draft, María Ángeles Tormo-Más: Investigation; Funding acquisition, Writing - review & editing , Javier Pemán: Investigation; Writing - review & editing, Félix Sancenón: Investigation; Supervision, Elena Aznar: Conceptualization; Funding acquisition, Writing - review & editing, Ramón Martínez-Máñez: Conceptualization, Funding acquisition, Writing - review & editing

## References

[1] Lai, H. Z., Wang, S. G., Wu, C. Y., Chen, Y. C., 2015. Anal Chem. 87, 2114-2120.

[2] Cheng, J. C., Huang, C. L., Lin, C. C., Chen, C. C., Chang, Y. C., Chang, S. S., Tseng, C. P., 2006. Clin. Chem. 52, 1997-2004.

[3] Moore, D. F., Curry, J. I., 1998. J. Clin. Microbiol. 36, 1028-1031.

[4] Edman, C. F., Mehta, P., Press, R., Spargo, C. A., Walker, G. T., Nerenberg, M., 2000. J. Invest. Med. 48, 93-101.

[5] Chang, T. C., Huang, S. H., 1994. J. Food Protect. 57, 184-189.

[6] Vigneshvar, S., Sudhakumari, C. C., Senthilkumaran, B., Prakash, H., 2016 Front. Bioeng. Biotechnol. 4, 11-20.

[7] Girigoswami, K., Akhtar, N., 2019. Int. J. Nano. Dimens. 10, 1-17.

[8] Abbaspour, A., Norouz-Sarvestani, F., Noori, A., Soltani, N., 2015. Biosens. Bioelectron. 68, 149-155.

[9] Wang, J., Wu, X., Wang, C., Shao, N., Dong, P., Xiao, R., Wang, S., 2015. ACS Appl. Mater. Interfaces 7, 20919-20929.

[10] Felix, F.S., Angnes, L., 2018. Biosens. Bioelectron. 102, 470-478.

[11] Luppa, P. B., Sokoll, L. J., Chan, D. W., 2001. Clin Chim Acta 314, 1-26.

[12] Lim, Y. C., Kouzani, A. Z., Duan, W., 2010. J. Biomed. Nanotech. 6, 93-105.

[13] Feng, C., Dai, S., Wang, L., 2014. Biosens. Bioelectron. 59, 64-74.

[14] O'Sullivan, C. K., 2002. Anal. Bioanal. Chem. 72, 44-48.

[15] Leca-Bouvier, B., Blum, L. J., 2005. Anal. Lett. 38, 1491-1517.

[16] Kim, Y. S., Gu, M. B., 2013. Biosensors Based on Aptamers and Enzymes, Springer, Berlin, Heidelberg.

[17] Aznar, E., Oroval, M., Pascual, L., Murguía, J. R., Martinez-Máñez, R., Sancenon, F., 2016. Chem. Rev. 116, 561-718.

[18] Sancenón, F., Pascual, L., Oroval, M., Aznar, E., Martinez-Máñez, R., 2015. ChemistryOpen 4, 418-437.

[19] Zelada-Guillén, G. A., Sebastián-Avila, J. L., Blondeau, P., Riu, J., Rius, F. X., 2012. Biosens. Bioelectron. 31, 226-232.

[20] Castillo, R. R., Baeza, A., Vallet-Regí, M., 2017. Biomater. Sci. 5, 353-377.

[21] Kurt, H., Yüce, M., Hussain, B., Budak, H., 2016. Biosens. Bioelectron. 81, 280-286.

[22] Lai, H. Z., Wang, S. G., Wu, C. Y., Chen, Y. C., 2015. Anal. Chem. 87, 2114-2120.

[23] Chang, Y. C., Yang, C. Y., Sun, R. L., Cheng, Y. F., Kao, W. C., Yang, P. C., 2013. Sci. Rep. 3, 1863-1870.

[24] Borsa, B. A., Tuna, B. G., Hernandez, F. J., Hernandez, L. I., Bayramoglu, G., Arica, M. Y., Ozalp, V. C., 2016. Biosens. Bioelectron. 86, 27-32.

[25] Otri, I., El Sayed, S., Medaglia, S., Martínez-Máñez, R., Aznar, E., Sancenón, F., 2019. Chem. Eur. J. 25, 3770-3774.

[26] Pascual, L., Baroja, I., Aznar, E., Sancenón, F., Marcos, M. D., Murguía, J.R., Amorós, P., Rurack, K., Martínez-Máñez, R., 2015. Chem. Commun., 51, 1414-1416.

[27] Ribes, À., Santiago-Felipe, S., Bernardos, A., Marcos, M.D., Pardo, T., Sancenón, F., Martínez-Máñez, R., Aznar, E., 2017. ChemistryOpen 6, 653-659.

[28] Chen, Y., Santos, A., Wang, Y., Kumeria, T., Li, J., Wang, C., Losic, D., 2015. ACS Appl. Mater. Interfaces 7, 19816-19824.

[29] Losic, D., Santos, A., 2015. Nanoporous Alumina: Fabrication, Structure, Properties and Applications, Springer Series in Materials Science, Springer International Publishing Switzerland.

[30] De la Escosura-Muniz, A., Merkoci, A., 2012. Acs Nano 6, 7556-7583.

[31] Baranowska, M., Slota, A. J., Eravuchira, P. J., Macias, G., Xifré-Pérez, E., Pallares, J., Ferré-Borrull, J., Marsal, L. F., 2014. Colloids Surf., B. 122, 375-383.

[32] Ribes, A., Xifré-Pérez, E., Aznar, E., Sancenón, F., Pardo, T., Marsal, L. F., Martínez-Máñez, R., 2016. Sci. Rep. 6, 38649.

[33] Pla, L., Xifré-Pérez, E., Ribes, A., Aznar, E., Marcos, M. D., Marsal, L. F., Martínez-Máñez, R., Sancenón, F., 2017. ChemPlusChem 82, 337-341.

[34] Ribes, À., Aznar, E., Santiago-Felipe, S., Xifré-Perez, E., Tormo-Mas, M. A., Pemán, J., Marsal, L. F., Martínez-Máñez, R., 2019. ACS Sensors 5, 1291-1298.

[35] Kreiswirth, B. N., Löfdahl, S., Betley, M. J., O'reilly, M., Schlievert, P. M., Bergdoll, M. S., Novick, R. P., 1983. Nature, 305, 709-712.

[36] Laboratory collection of diverse species of Staphylococcus obtained under the approval of the Ethic Committee of Hospital Universitario y Politécnico La Fe (2017/0523) for project SAF2017-82251-R.

[37] Christensen, G. D., Simpson, W. A., Bisno, A. L., Beachey, E. H., 1982. Infect Immun. 37, 318-326.

[38] Wagner, E., Doskar, J., Götz, F., 1998. Microbiology 144, 509-517.

[39] Tormo, M. A., Knecht, E., Götz, F., Lasa, I., Penades, J. R., 2005. Microbiology 151, 2465-2475.

[40] Oliveira, K., Procop, G. W., Wilson, D., Coull, J., Stender, H., 2002. J. Clin. Microbiol., 40, 247-251.

[41] Song, Z., Liu, X., Zhu, M., Tan, Y., Wu, K., 2017. Mol. Vis. 23, 407-415.

[42] Marlowe, E. M., Bankowski, M. J., 2011. J. Clin. Microbiol. 49, S53-S59.

[43] Huang, S. H., Chang, T. C., 2004. Clin. Chem. 50, 1673-1674.

[44] Burghardt, E. L., Flenker, K. S., Clark, K. C., Miguel, J., Ince, D., Winokur, P., McNamara, J. O., 2016. PloS one 11, e0157234.